nature synthesis

Article

https://doi.org/10.1038/s44160-024-00637-y

Light-enabled scalable synthesis of bicyclo[1.1.1]pentane halides and their functionalizations

Received: 9 September 2023

Accepted: 2 August 2024

Published online: 5 September 2024

Check for updates

Vasyl Ripenko[1], Vadym Sham[1], Vitalina Levchenko[1], Serhii Holovchuk[1], Daniil Vysochyn[1], Ivan Klymov[1], Dmytro Kyslyi[1], Stanislav Veselovych[1], Serhii Zhersh[1], Yurii Dmytriv[1,2], Andrey Tolmachev[1], Iryna Sadkova[1], Irina Pishel[3], Kateryna Horbatok[3], Viktoria Kosach[3], Yelyzaveta Nikandrova[3] & Pavel K. Mykhailiuk[1]

In 2012, bicyclo[1.1.1]pentanes were demonstrated to be bioisosteres of the benzene ring. Here, we report a general scalable reaction between alkyl iodides and propellane that provides bicyclo[1.1.1]pentane iodides in milligram, gram and even kilogram quantities. The reaction is performed in flow and requires just light; no catalysts, initiators or additives are needed. The reaction is clean enough that, in many cases, evaporation of the reaction mixture provides products in around 90% purity that can be directly used in further transformations without any purification. Combined with the subsequent functionalization, >300 bicyclo[1.1.1]pentanes for medicinal chemistry have been prepared. So far, this is the most general and scalable approach towards functionalized bicyclo[1.1.1]pentanes.

The benzene ring is the most popular ring in drugs[1,2] and natural products[3]. In 2012, bicyclo[1.1.1]pentane (BCP) was demonstrated to mimic the *para*-substituted benzene ring in a biologically active compound (Fig. 1a)[4]. Since then, BCPs have been playing an important role in chemistry[5–32]. Synthesis and applications of BCPs are covered in at least ten recent reviews[5–14]. Moreover, >300 patents describe an application of BCPs in drug discovery projects (Fig. 1b). Most of these compounds bear a (hetero)aromatic substituent, the hydrogen atom or a carboxylic group derivative at the bridgehead position of the BCP core, however, alkyl substituents are rare.

Worth specific mentioning is a recent collaboration between Pfizer and the Baran laboratory on developing a scalable 'strain-release' amination of propellane[33,34]. This study allowed the preparation of BCP amines with no substituents at the bridgehead position.

Aliphatic substituents increase the fraction of sp^3-hybridized carbon atoms ($F(sp^3)$) in bioactive molecules and, therefore, it is not surprising that medicinal chemists favour using them nowadays[35,36]. In this context, alkyl-substituted BCPs are conceptually interesting, yet almost unknown.

In this work, we have developed a general scalable reaction between inexpensive starting materials—alkyl iodides and propellane—that gives alkyl-substituted BCP iodides in milligram, gram and even kilogram quantities. The reaction proceeds in flow and requires only light. No catalysts, initiators or additives are needed. The transformation is so clean that in many cases, evaporation of the reaction mixture provides products in around 90% purity that can be directly used in the next steps without any purification. The subsequent modifications of the obtained products allowed the preparation of >300 BCP building blocks for use in medicinal chemistry. So far, this is the most general and scalable approach towards functionalized BCPs.

Results

Optimization

In a search for a general scalable method towards alkyl-substituted BCPs, we focused our attention on the reaction of alkyl iodides with propellane. In 1991, this reaction was shown to take place under irradiation with a broad-wavelength Hanovia mercury lamp in a Pyrex vessel (Fig. 1c)[37]. In 2000, it was demonstrated that the addition of

[1]Enamine Ltd., Kyiv, Ukraine. [2]National Technical University of Ukraine, Igor Sikorsky Kyiv Polytechnic Institute, Kyiv, Ukraine. [3]Bienta, Kyiv, Ukraine. e-mail: pavel.mykhailiuk@gmail.com

https://doi.org/10.1038/s44160-024-00637-y

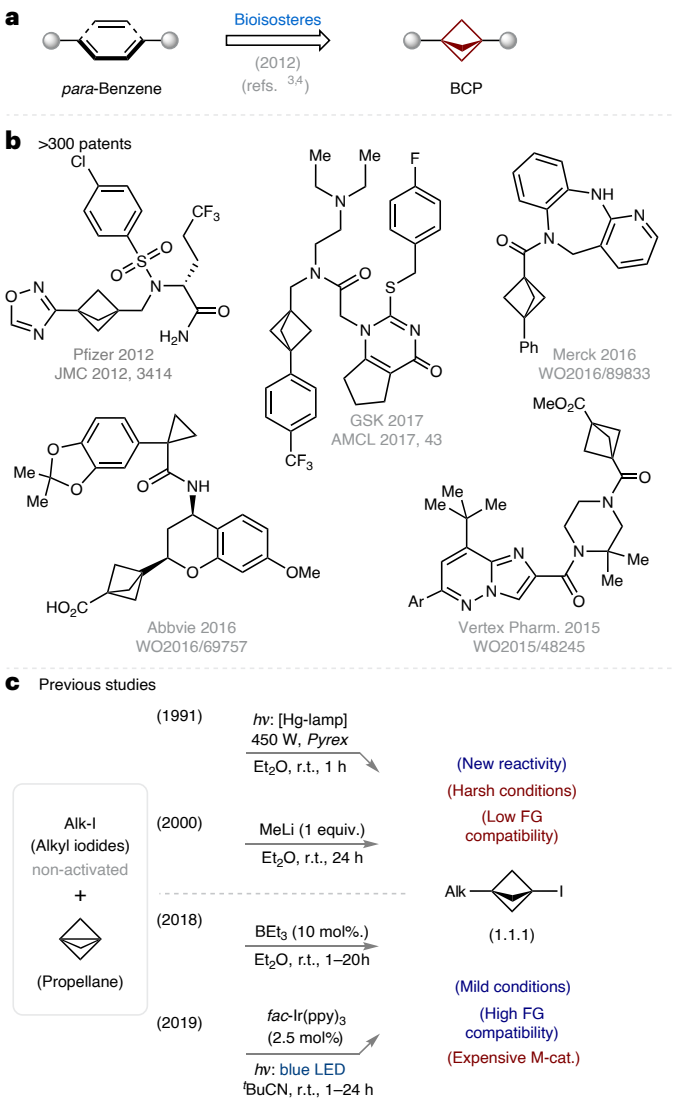

Fig. 1 | Application and synthesis of BCPs. a, The concept begins with BCPs as saturated bioisosteres of the *para*-substituted benzene ring[3,4]. **b**, BCPs in drug discovery projects. In the first two molecules (Pfizer in 2012, ref. 4 and GlaxoSmithKline (GSK) in 2017, ref. 16) BCPs have been used as saturated benzene bioisosteres. **c**, Known approaches to alkyl-substituted BCP iodides. r.t., room temperature; *fac*-Ir(ppy)$_3$, *fac-tris*(2-phenylpyridine)iridium(III); FG, functional group.

an equimolar amount of methyl lithium also promoted the reaction (Fig. 1c)[38]. The challenges associated with the ultraviolet irradiation in Pyrex glassware and the low compatibility of methyl lithium with various functional groups lowered the practical potential of both methods[39–43]. In 2018, scientists discovered that triethylborane initiated the reaction leading to the formation of products in good yields (Fig. 1c)[44–46]. In 2019, the reaction scope was improved by performing the reaction in the presence of the *fac*-Ir(ppy)$_3$ catalyst under the photoredox conditions[47,48]. The key disadvantage of the last method was the relatively high price of the metal catalyst (price of *fac*-Ir(ppy)$_3$ (Aldrich): €852 for 250 mg). It is worth noting that some activated alkyl iodides, such as CF_3I, HCF_2I and EtO_2CCF_2I, were reported to react with propellane at room temperature without any initiation or catalysis[49–51]. The reaction was slow, and typically took place over 48–72 hours.

Known approaches towards alkyl-substituted BCPs are depicted in Fig. 1c. These reactions were described on a milligram scale. Therefore, we first tried these protocols on a gram scale with the most challenging

Table 1 | Optimization of synthesis of BCP 1

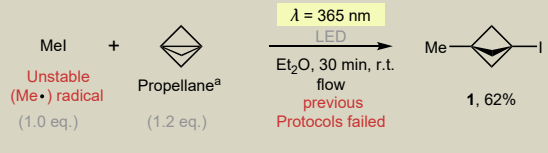

Entry	Conditions	Yield (%)[b]
1	MeLi (1 eq.), r.t., 24 h	5
2	I_2 (0.25% mol.), r.t., 24 h	16
3	BEt_3 (10% mol.), Et_2O, r.t., 24 h	31
4	*fac*-Ir(ppy)$_3$ (2.5% mol.), Et_2O, 450 nm, 12 h	Polymerization
5	*fac*-Ir(ppy)$_3$ (2.5% mol.), ^{t}BuCN, 450 nm, 12 h	Polymerization
6	*fac*-Ir(ppy)$_3$ (2.5% mol.), ^{t}BuCN, 450 nm, 12 h (2 eq. propellane)	14
7	254 nm, Et_2O, r.t., 24 h, in batch	12
8	310 nm, Et_2O, r.t., 24 h, in batch	17
9	450 nm, Et_2O, r.t., 24 h, in batch	<5
10	365 nm, Et_2O, r.t., 24 h, in batch	43
11	365 nm, Et_2O, r.t., 30 min, in flow	62
12	365 nm, Et_2O, r.t., 30 min, in flow (2 eq. MeI)	73
13	365 nm, MeO^{t}Bu, r.t., 30 min, in flow	51
14	r.t., 30 min (control)	ND
15	r.t., 24 h (control)	6[c]
16	365 nm, Et_2O, r.t., in flow (855 g of product)	72[c]

Scale, 10 g of MeI in each experiment. ND, not detected. [a]Solution of propellane (0.7 M) in Et_2O-$CH_2(OEt)_2$. [b]Isolated yield. Distillation as a purification method. [c]Crystallization as a purification method.

alkyl substrate: methyl iodide (MeI). The methyl radical is the most unstable among all common alkyl radicals. We thought that if we could elaborate on a scalable protocol for the reaction of MeI, it would work with other alkyl iodides too.

The reaction of MeI with propellane (1.2 eq.) in the presence of methyl lithium[37] or iodine gave only traces of the needed product **1** (Table 1, entries 1 and 2). Initiation with BEt_3 (ref. 44) gave the product **1** in 31% yield, however, an extensive formation of polymeric products was observed (entry 3). Catalysis with *fac*-Ir(ppy)$_3$ (refs. 45,46) led to the formation of a complex mixture (entries 4 and 5). With an excess of propellane (2 eq.), however, we obtained iodide **1** in 14% yield. Next, we attempted the reaction under various photochemical conditions in batch with no catalysts/initiators (entries 7–10). Irradiation of the reaction mixture at 254 or 310 nm gave <20% of the needed product (entries 7 and 8). Irradiation at 450 nm (blue light-emitting diode (LED)) did not promote the reaction (entry 9). However, the irradiation at 365 nm in batch allowed obtaining the desired product **1** in 43% yield (entry 10). After further optimization, we found that performing the reaction in flow for 30 minutes allowed increasing the yield to 62% (entry 11).

It is worth noting that all experiments in entries 1–11 (Table 1) were performed under the standard conditions: MeI (10 g; 1 eq.) and propellane (1.2 eq.). In each case, the product was isolated by distillation under reduced pressure. Moreover, performing the reaction with an excess of MeI (2 eq.) led to an improvement of the yield to 73% (entry 12). However, because many alkyl iodides are expensive, for further studies we used the reaction conditions that require an almost equimolar amount of reagents (entry 11).

https://doi.org/10.1038/s44160-024-00637-y

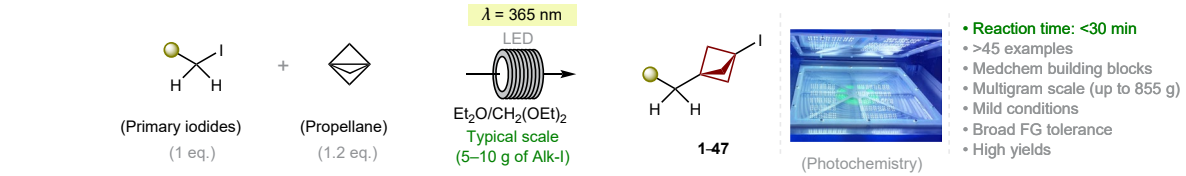

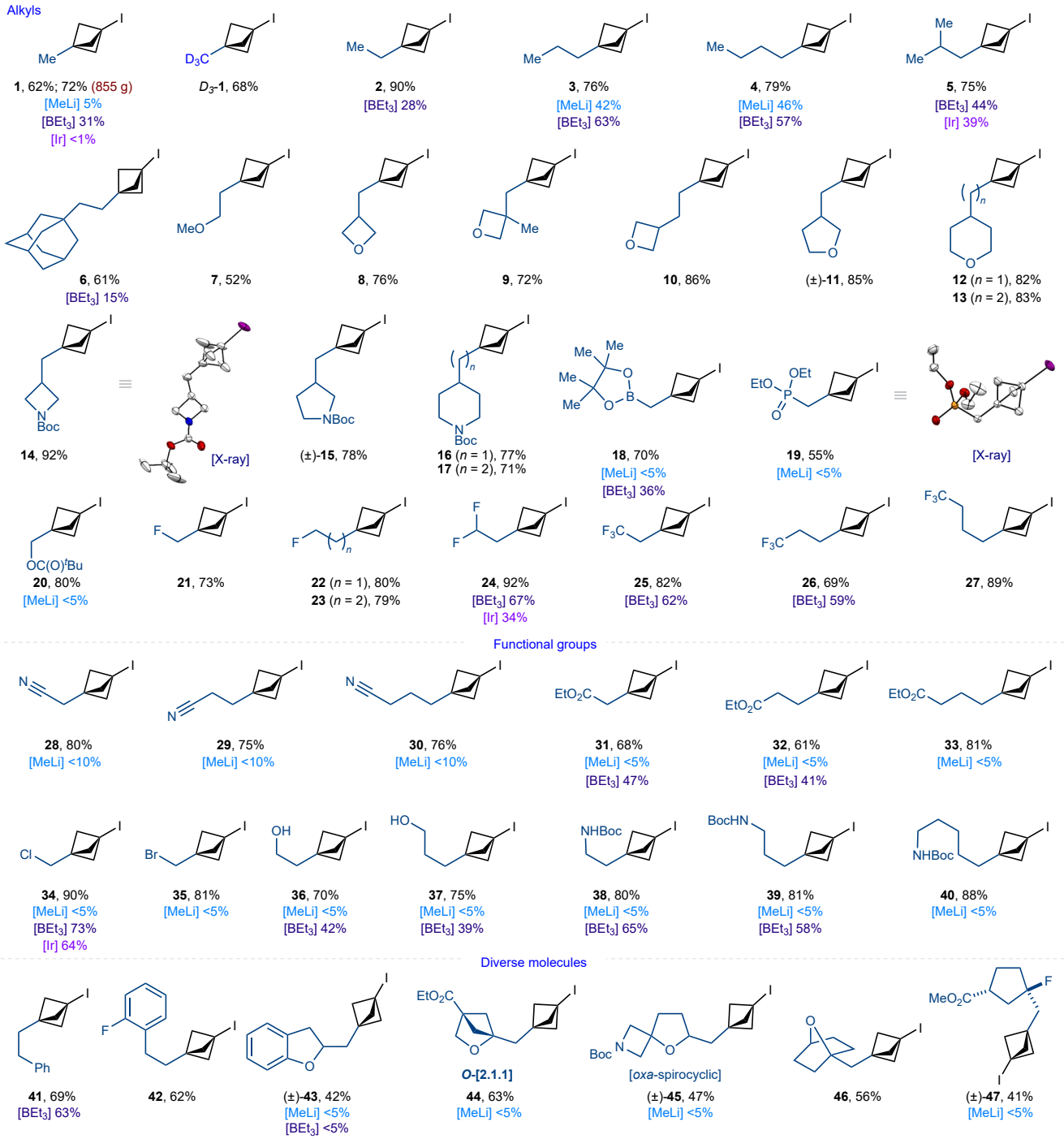

Fig. 2 | Synthesis of BCPs from primary alkyl iodides. Reaction conditions were as follows: a solution of alkyl iodide (1 eq.) and propellane (0.7 M in Et_2O/$CH_2(OEt)_2$; 1.2 eq.) in diethyl ether was passed through a coil (irradiated area 160 ml) with a flow rate 10 ml min^{-1} under irradiation with 365 nm LED (radiated power 420 W). Residence time was 16 min. Typical scale was 5–10 g of alkyl iodide. Compounds **1**, **2** and **22** were additionally obtained on a multigram scale. Synthesis of compounds **6**, **40**, **42**–**47** was performed on 0.1–2 g scale (irradiated coil 7.6 ml; flow rate 0.75 ml min^{-1}; irradiation 365 nm LED; radiated power 257 W and residence time 10.1 min). [MeLi]: MeLi (1 eq.), $CH_2(OEt)_2$, 24 h, r.t., in batch. [BEt_3]: BEt_3 (0.1 eq.), Et_2O, 24 h, r.t., in batch; [Ir].*fac*-Ir(ppy)$_3$ (2.5% mol.), ^{t}BuCN, 12 h, r.t., in batch. X-ray crystal structure of compounds **14** and **19**. Hydrogen atoms are omitted for clarity. Boc, *tert*-butoxycarbonyl protecting group.

https://doi.org/10.1038/s44160-024-00637-y

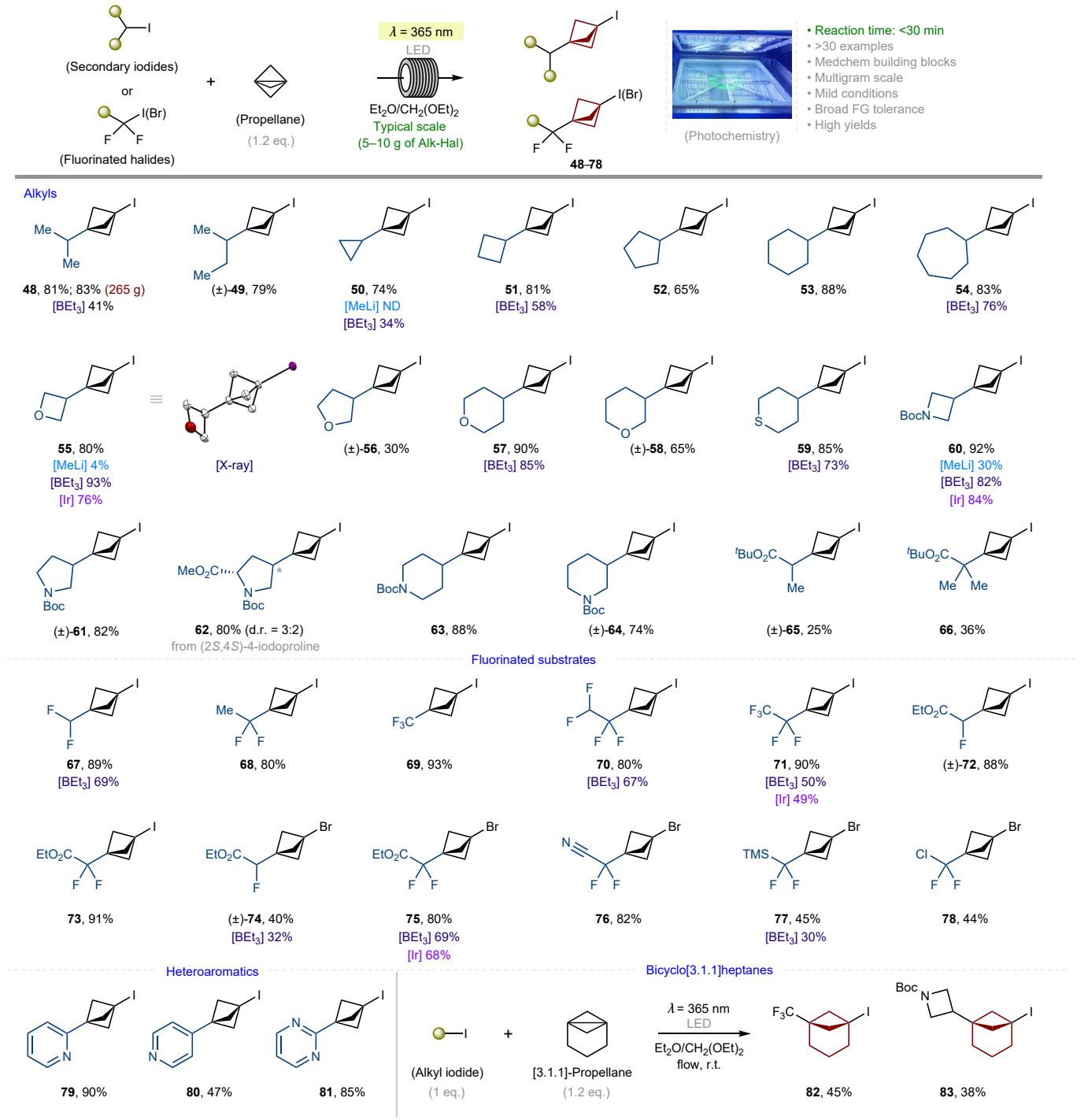

Fig. 3 | Synthesis of BCP halides and bicyclo[3.1.1]heptanes. Reaction conditions were as follows: a solution of alkyl iodide (1 eq.) and propellane (0.7 M in $Et_2O/CH_2(OEt)_2$; 1.2 eq.) in diethyl ether was passed through a coil (irradiated area 160 ml) with a flow rate 10 ml min^{-1} under irradiation with 365 nm LED (radiated power 420 W). Residence time was 16 min. Typical scale 5–10 g of alkyl iodide. Compounds **48**, **60** and **63** were also obtained on a multigram scale. [MeLi]: MeLi (1 eq.), $CH_2(OEt)_2$, 24 h, r.t., in batch; [BEt_3]: BEt_3 (0.1 eq.), Et_2O, 24 h, r.t., in batch; [Ir]: *fac*-Ir(ppy)$_3$ (2.5% mol.), ^{t}BuCN, 15 h, r.t., in batch. X-ray crystal structure of compound **55**. Hydrogen atoms are omitted for clarity.

It is important to mention that propellane can also be synthesized in MeO^{t}Bu instead of Et_2O (also Supplementary Information, page 27). Its reaction with MeI under the developed conditions also worked and provided product **1** in 51% yield (entry 13).

Control experiments revealed that without irradiation the reaction of MeI with propellane did not proceed efficiently (entries 14, 15).

Having an optimized protocol in hand (Table 1, entry 11), we synthesized pure BCP **1** in 855 g amount in one run with almost no additional modifications (Table 1, entry 16; also Supplementary Information, pages 62–63). In this case, however, we isolated the product (72% yield) from the reaction mixture by a low-temperature crystallization from pentane.

Scope

Next, we studied the generality of the developed method. First, we tried other primary alkyl iodides (Fig. 2). Given the rise of deuterated compounds in modern drug discovery[52,53], we performed an addition of CD_3I to propellane under standard conditions to obtain product

D_3-**1** in 68% yield. The reaction worked well with other alkyl iodides (**3**–**7**), oxetane-containing substrates (**8**–**10**), tetrahydrofuran (**11**) and tetrahydropyran-containing molecules (**12**,**13**). *N*-Boc-protected azetidines (**14**), pyrrolidines (**15**) and piperidines (**16**,**17**) performed equally well in the reaction. In addition, Bpin (**18**), $PO(OEt)_2$ (**19**) and ^{t}BuC(O)O groups (**20**) were compatible with the reaction conditions. Given the importance of organofluorine compounds in modern medicinal chemistry[54–56], we performed the reaction with various fluorinated alkyl iodides to obtain BCPs **21**–**27** in 69–92% yield. The structure of products **14** and **19** was confirmed by X-ray analysis.

Various functional groups, such as nitrile (**28**–**30**), ester (**31**–**33**), active chlorine (**34**) and bromine atoms (**35**), alcohol (**36**, **37**) and NHBoc (**38**–**40**) were compatible with the reaction conditions. Diverse cores including 2-oxabicyclo[2.1.1]hexane (**44**)[57–59] and oxa-spirocycles (**45**)[60] also gave the desired BCP iodides **41**–**47** in 41–69% yield.

We also studied the behaviour of secondary alkyl iodides (Fig. 3). The protocol efficiently worked for isopropyl (**48**), isobutyl (**49**) and cycloalkyl (**50**–**54**) iodides.

Four-to-six-membered rings with oxygen (**55**–**58**), sulfur (**59**) and *N*-Boc (**60**–**64**) gave the desired products in 30–92% yield. Secondary, $MeCH(I)CO_2{}^tBu$, and tertiary, $Me_2C(I)CO_2{}^tBu$, iodides also reacted with propellane to provide products **65**, **66** in lower yields of 25–36% due to a problematic purification[61]. Various fluoroalkyl iodides (**67**–**73**) and even bromides (**74**–**78**)[62] were compatible with the reaction conditions too. The structure of product **55** was confirmed by X-ray analysis.

Several representative (hetero)aromatic iodides also were subjected to the standard reaction conditions, and products **79**–**81** were obtained in 47–90% yield. Phenyl iodide did not react, however.

Recently, bicyclo[3.1.1]heptanes were proposed to mimic the *meta*-substituted benzene ring in bioactive compounds[63]. In this context, we studied the reaction of [3.1.1]-propellane with two representative alkyl iodides under the above-developed conditions. The desired bicyclo[3.1.1]heptanes **82** (45%) and **83** (38%) were obtained as a result of these efforts (Fig. 3).

Scalability

Most of the syntheses depicted in Figs. 2 and 3 were performed with 5–10 g of starting alkyl iodides. The typical reaction time was less than 30 minutes. Only syntheses of BCPs **6**, **40**, **42**–**47** were performed on a smaller scale due to the low availability of the corresponding alkyl iodides.

For many examined substrates, we compared the performance of our conditions with the literature protocols on the same scale (Figs. 2 and 3). MeLi gave poor yields of the desired products bearing functional groups; initiation with triethylborane often gave good results (**3**–**5**, **55**, **57**, **60** and so on). In each case, however, a standard aqueous workup followed by purification by column chromatography or distillation was needed.

The photochemical protocol developed here gave the best yields of products in all cases, where different protocols were examined and compared. In many cases, the reaction was so clean that evaporation of the reaction mixture provided products with around 90% purity that can be directly used in the next steps without any purification. It allowed us therefore to subsequently scale up the preparation of BCP iodides **1**–**3**, **5**, **7**, **14**–**16**, **21**–**27**, **48**, **50**, **55**, **57**, **59**–**63**, **67**–**69**, **71**, **75** and **77** to 50–800 g quantities (also Supplementary Information, pages 62–70).

Mechanism

Product **62** (Fig. 3) was obtained from the derivative of the optically pure (2*S*,4*S*)-4-iodoproline as a 3:2 mixture of two diastereomers at *C*(4)-atom (Fig. 3). This observation suggested the radical mechanism of the reaction with the initial photochemical formation of the configurationally unstable alkyl radicals. To validate this hypothesis, we performed 'radical clock' experiments (also Supplementary Information, pages 71–87)[64]. Alkyl iodide **84** was reacted with propellane under the developed conditions to selectively form the ring-opened alkene **85** (Fig. 4). In the nuclear magnetic resonance (NMR) spectroscopy of the crude reaction mixture, we did not observe even traces of the cyclopropane ring. In the presence of (2,2,6,6-tetramethylpiperidin-1-yl)oxyl (TEMPO), the formation of product **85** was not observed. In the absence of propellane, an isomerization of iodide **84** into compound **86** slowly took place. Similarly, the reaction of alkyl iodide **87** with propellane gave mostly the rearranged cyclopentane-containing product **88** with only traces of alkene **89** (**88**:**89** = 5:1, Fig. 4). These experiments supported the original hypothesis of the radical pathway of the reaction.

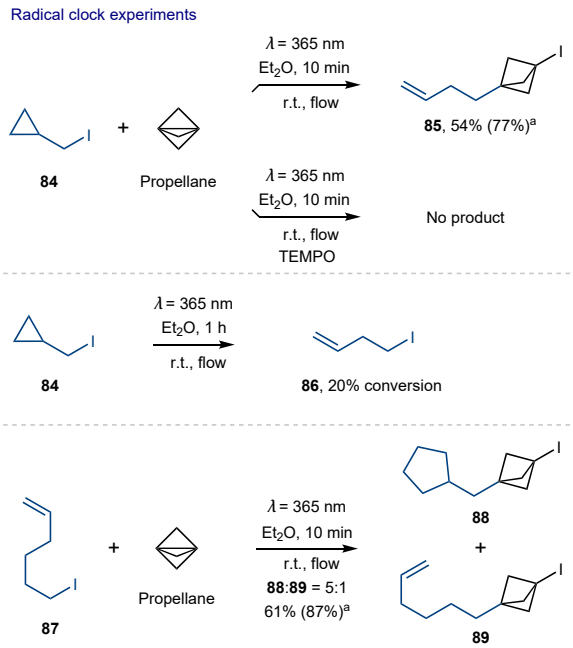

Fig. 4 | Radical clock experiments with alkyl iodides 84 and 87. [a]NMR yield using 1,3,5-trimethoxybenzene as an internal standard.

Modifications

Having a practical and scalable protocol towards alkyl BCP iodides in hand, we converted them into various BCP-containing building blocks (compounds with one or two functional groups) for use in medicinal chemistry. Treatment of BCP iodides with *t*-BuLi in Et_2O followed by trapping of the formed carbanions with (^{i}PrO)Bpin gave boron pinacolates **a** (Fig. 5)[65–73]. The reaction of the last with potassium fluoride in an acetone–water mixture smoothly gave trifluoroborates **b**. Oxidation of boron pinacolates with H_2O_2 gave alcohols **c** (ref. 74). Trapping of BCP-carbanions with diverse electrophiles was also studied. Reaction with BocN=N-Boc followed by the acidic *N*-Boc deprotection produced hydrazines **d** (Fig. 5)[75,76]. Reaction with sulfur dioxide followed by the oxidative chlorination of the intermediate sulfinate salts gave sulfonyl chlorides **e** (refs. 77–81). Reaction with hexachloroethane afforded BCP chlorides **f**. An analogous reaction with 1,1,2,2-tetrabromo-1,2-difluoroethane provided BCP-bromides **g**. The addition of CD_3OD followed by the *N*-Boc deprotection gave deuterated amines **60h** and **63h**. The addition of ethyl formate gave aldehydes **i**. Treatment of carbanions with methanol followed by optional hydrolysis of the ester group or the *N*-Boc deprotection gave *mono*-substituted BCPs: carboxylic acids, amines and alcohols **j**. Reaction with dry ice gave carboxylic acids **k** (refs. 82–101). Standard Curtius reactions of the last gave amines **l** (refs. 83,102–106).

The obtained BCP iodides were also compatible with radical cross-couplings. Several successful representative [Fe]- and [Cu]-catalysed reactions[107,108] of iodide **1** with ArMgCl and *N*-azoles were performed to

https://doi.org/10.1038/s44160-024-00637-y

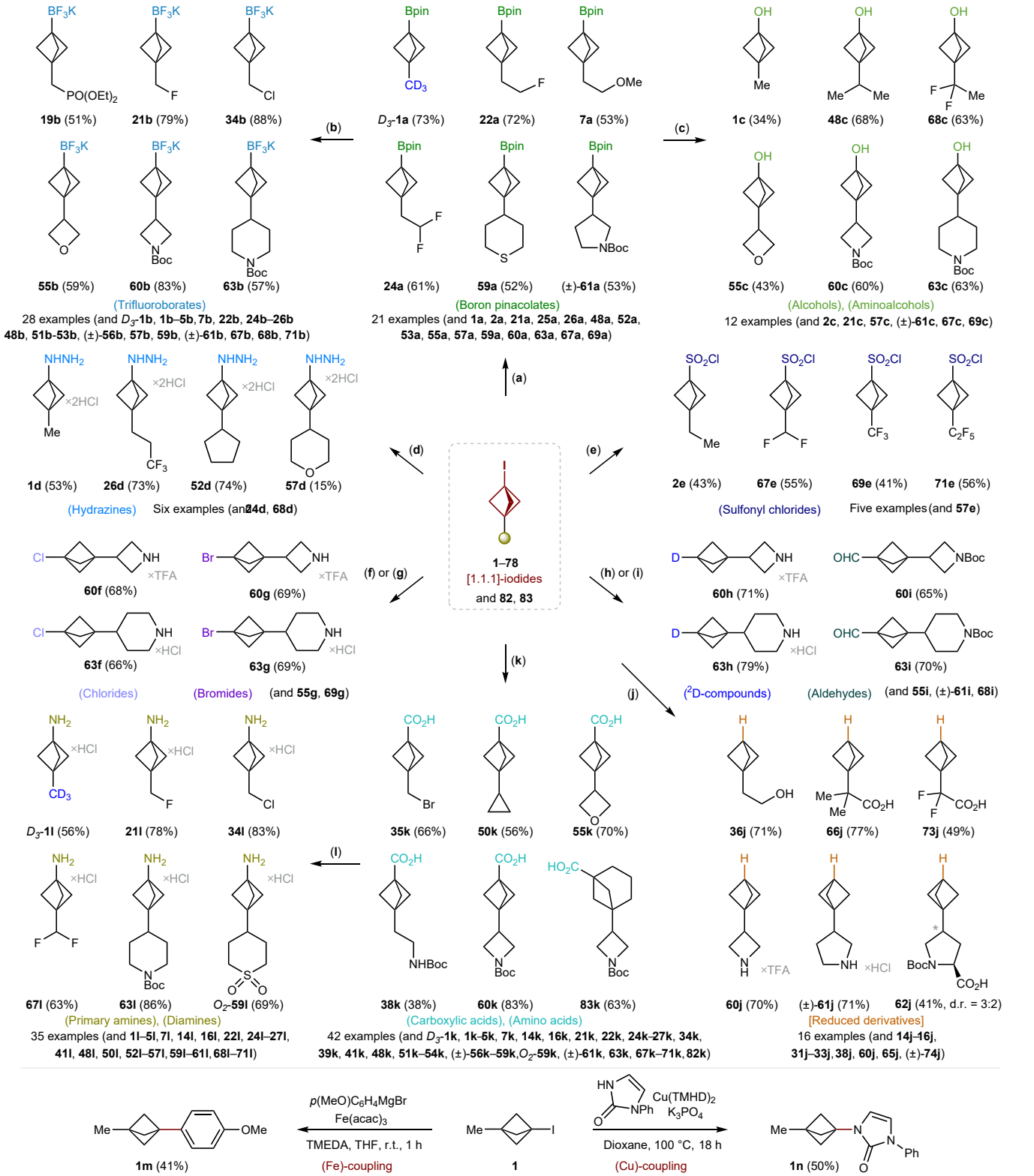

Fig. 5 | Modifications of BCP and bicyclo[3.1.1]heptane iodides. Reaction conditions for all conditions are shown. **a**, (^{i}PrO)Bpin, *t*-BuLi, Et_2O, −100 °C. **b**, KHF_2, acetone–water, r.t. **c**, KH_2PO_4, H_2O_2, THF–water, r.t. **d**, (i) BocN=N-Boc, *t*-BuLi, Et_2O, −100 °C; (ii) dioxane-HCl, r.t. **e**, (i) *t*-BuLi, SO_2, Et_2O; (ii) Cl_2, CH_2Cl_2–H_2O, 0–5 °C. **f**, (i) *t*-BuLi, Cl_3CCCl_3, Et_2O, −100 °C; (ii) deprotection: HCl–dioxane or TFA–CH_2Cl_2. **g**, (i) *t*-BuLi, $C_2Br_2F_4$, Et_2O, −100 °C; (ii) deprotection: HCl–dioxane or TFA–CH_2Cl_2. **h**, (i) *t*-BuLi, CD_3OD, Et_2O, −100 °C; (ii) deprotection: HCl–dioxane or TFA–CH_2Cl_2. **i**, *t*-BuLi, ethyl formate, Et_2O, −100 °C. **j**, Four methods for the reduction of the C-I bond: *t*-BuLi, MeOH, Et_2O, −100 °C; Raney-Ni, EtOH, ethylenediamine, r.t.; Bu_3SnH, AIBN, CCl_4, r.t.; or Pd–C, H_2, NEt_3, MeOH, r.t. **k**, *t*-BuLi, CO_2, Et_2O, −80 °C. **l**, (i) $(PhO)_2P(O)N_3$, Et_3N, *t*-BuOH, 95 °C; (ii) HCl–dioxane, Et_2O, r.t. Bpin, 4,4,5,5-tetramethyl-1,3,2-dioxaborolane; TFA, trifluoroacetic acid; acac, acetylacetonate; AIBN, azobisisobutyronitrile; $Cu(TMHD)_2$, copper *bis*(2,2,6,6-tetramethyl-3,5-heptanedionate); TMEDA, tetramethylethylenediamine.

https://doi.org/10.1038/s44160-024-00637-y

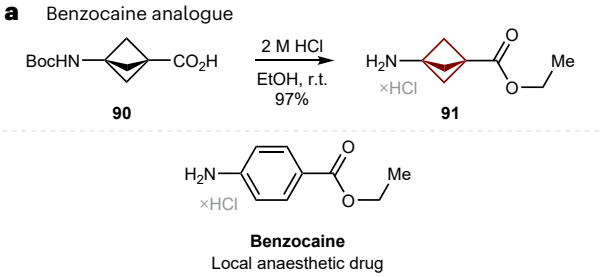

Compound	Sol.	clog*P*	log*D*	CL_{int}	$t_{1/2}$
Benzocaine	385	1.50	1.8	83	20
91	319	0.02	0.1	140	12

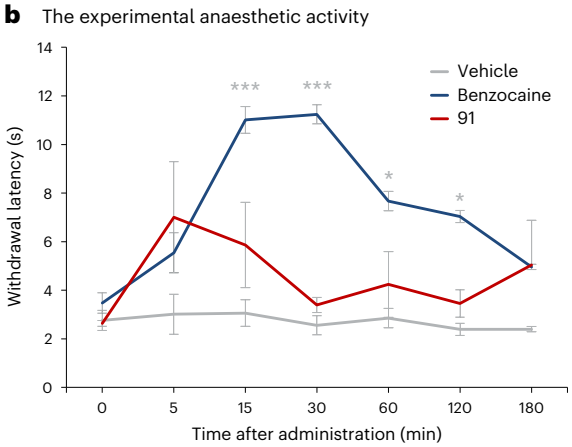

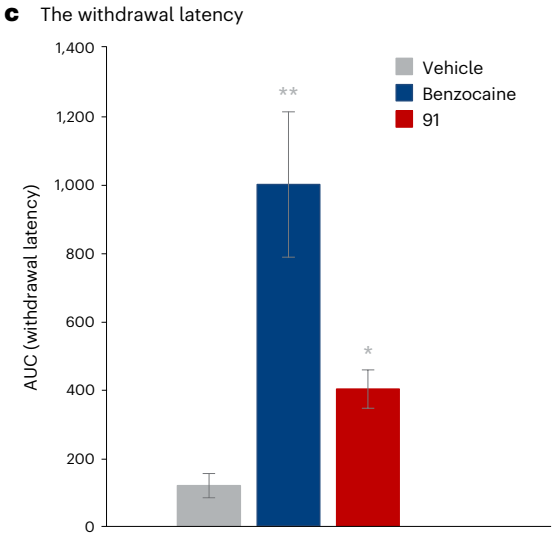

Fig. 6 | Synthesis, physicochemical properties and biological activity of Benzocaine analogue. a, Synthesis of saturated analogue of the local anaesthetic drug, Benzocaine, compound **91**. Sol., the experimental kinetic solubility in phosphate-buffered saline, pH 7.4 (μM). log*D* (7.4), the experimental distribution coefficient in *n*-octanol–phosphate-buffered saline, pH 7.4. clog*P*, the calculated lipophilicity. CL_{int}, the experimental metabolic stability in human liver microsomes (μl min^{-1} mg^{-1}). $t_{1/2}$ (min), the experimental half-time of a metabolic decomposition in human liver microsomes. **b**, Time course of the antinociceptive effect of Benzocaine and its analogue **91** in tail flick test. The data Are presented as mean ± s.e.m. ($n = 5$). *$P(t) < 0.05$ and ***$P(t) < 0.001$ compared with the control group (vehicle) data were analysed using a two-sided Student's *t*-test without multiple comparisons. **c**, The area under the curve (AUC) of the withdrawal latency of Benzocaine and its analogue **91** in a tail flick test[110]. The data were presented as mean ± s.e.m. ($n = 5$). *$P(t) = 0.026$; **$P(t) = 0.002$ compared with the control group (vehicle) data were analysed using a two-sided Student's *t*-test without multiple comparisons. *n*, sample size.

obtain products **1m** and **1n** (Fig. 5; see also Supplementary Information, pages 175–178 for other examples).

Using this strategy, we have prepared >200 functionalized BCPs in gram quantities (Fig. 5). So far, this is the most general and scalable approach to functionalized BCPs. Many of these molecules have already found an application in drug discovery projects (Supplementary Information, pages 182–187).

Replacement of benzene by BCP in drugs

To independently validate the BCP scaffold as a saturated benzene bioisostere[5–8], we aimed to incorporate it into existing drugs. We also planned to study the impact of such replacement at the experimental physicochemical properties and biological activity. We chose the FDA-approved local anaesthetic drug Benzocaine and the antihistamine drug Buclizine with the *para*-substituted benzene rings.

The synthesis of a saturated analogue of Benzocaine commenced from *N*-Boc amino acid **90**. Acidic *N*-Boc cleavage in ethanol and the simultaneous esterification of the carboxyl group gave the desired compound **91** as a hydrochloride salt (Fig. 6).

An impact of the replacement of the benzene ring in Benzocaine with BCP at the experimental physicochemical properties—water solubility, lipophilicity—and metabolic stability was investigated (Fig. 6). Such replacement slightly decreased the water solubility: 385 μM (Benzocaine) versus 319 (**91**). To estimate the influence of the replacement on lipophilicity, we used two parameters: calculated (clog*P*) (clog*P* was calculated with ChemAxon (v.22.13)) and experimental (log*D*) lipophilicities. According to both indices, the replacement of the benzene ring with BCP notably decreased the lipophilicity by ≥1.5 clog*P*/log*D* units. The replacement also decreased the metabolic stability, CL_{int} (mg min^{-1} μl^{-1}): 83 (Benzocaine) versus 140 (**91**).

We also measured the experimental anaesthetic activity of Benzocaine and its analogue **91** in vivo. We studied the antinociceptive effect of both compounds using the 'tail flick test'[109] in 2-month-old CD-1 female mice (Fig. 6 and Supplementary Information, pages 880–885. Study design, animal selection, handling and treatment were in accordance with Bienta Animal Care and Use Guidelines, and European Union directive 2010/63/EU). On the one hand, compound **91** was found to be less active compared to the original drug Benzocaine: no substantial difference in response time to tail flick was present throughout the observation period. On the other hand, analogue **91** demonstrated a clear analgesic activity: a notable increase in coverage of analgesia by time (area under the curve level) compared to that of the vehicle (Fig. 6).

The synthesis of a saturated analogue of Buclizine was performed from the carboxylic acid **92**. Amide coupling of the latter with the appropriately *N*-substituted piperazine provided compound **93**. Reduction of the amide group with $LiAlH_4$ followed by addition of hydrochloric acid gave the desired compound **94** as a hydrochloride salt (Fig. 7).

Replacement of the benzene ring in Buclizine by BCP (**94**) did not affect its water solubility, as both compounds were poorly soluble in water: ≤1 μM (Fig. 7). The replacement substantially decreased the lipophilicity, however, by 1–2 clog*P*/log*D* units. An impact of the replacement on the metabolic stability was not observed, as both compounds had high stability, thus outside the reliable range for measurements (Fig. 7).

Buclizine is an antihistamine agent used as a drug for the treatment of allergy symptoms and the prevention of nausea and vomiting. Recently, Buclizine was suggested for repurposing for cancer treatment, following an observation that the original target (histamine-releasing factor) and the suggested one (translationally controlled tumour protein) were identical[110]. Subsequently, Buclizine was found to exhibit cytostatic effect in MCF-7 human cancer cell line. The cell growth arrest was observed in a suppression of cell respiration

https://doi.org/10.1038/s44160-024-00637-y

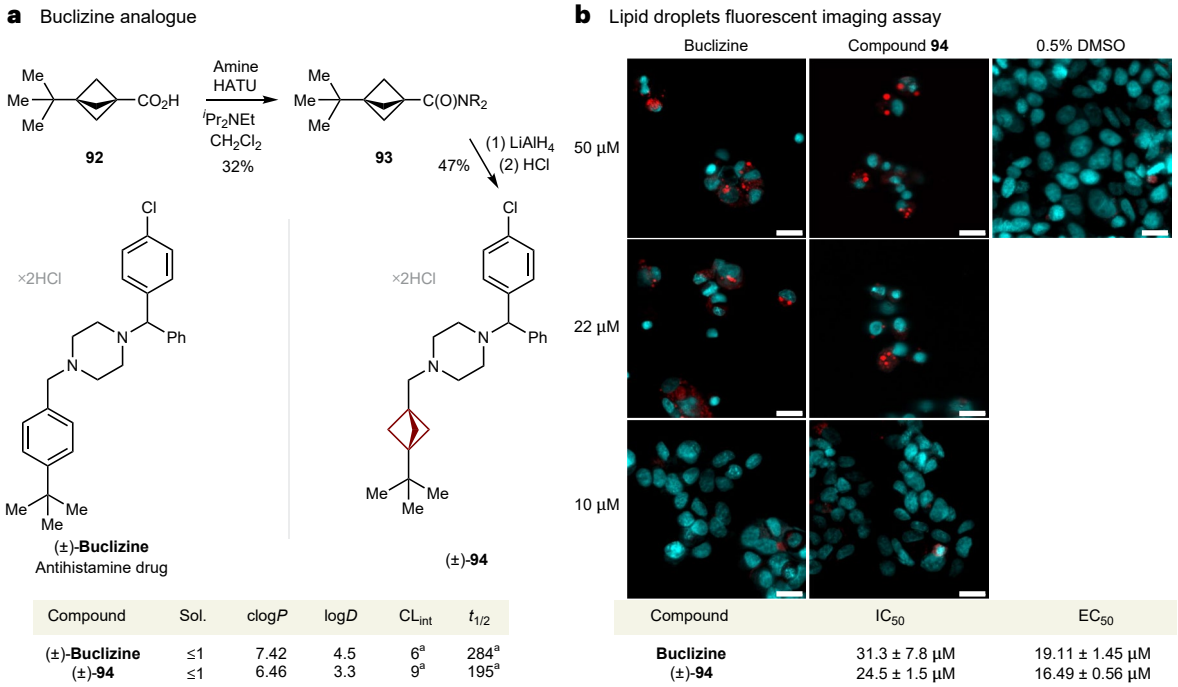

Compound	Sol.	clog*P*	log*D*	CL_{int}	$t_{1/2}$
(±)-**Buclizine**	≤1	7.42	4.5	6[a]	284[a]
(±)-**94**	≤1	6.46	3.3	9[a]	195[a]

Compound	IC_{50}	EC_{50}
Buclizine	31.3 ± 7.8 µM	19.11 ± 1.45 µM
(±)-**94**	24.5 ± 1.5 µM	16.49 ± 0.56 µM

Fig. 7 | Synthesis and lipid droplets fluorescent imaging assay of Buclizine analogue. a, Synthesis of saturated analogue of the antihistamine drug Buclizine, compound **94**. Sol., the experimental kinetic solubility in phosphate-buffered saline, pH 7.4 (µM). log*D* (7.4): the experimental distribution coefficient in *n*-octanol–phosphate-buffered saline, pH 7.4. clog*P*, the calculated lipophilicity. CL_{int}, the experimental metabolic stability in human liver microsomes (µl min^{-1} mg^{-1}). $t_{1/2}$ (min), the experimental half-time of a metabolic decomposition in human liver microsomes. [a]Parameter should be considered as approximate due to the high stability of compounds. **b**, Confocal images of the lipid droplet formation in MCF-7 cells on incubation with Buclizine and analogue **94** for 72 h. Nuclei were stained with Hoechst 33342 (cyan), lipid droplets were stained with Nile Red (red). Scale bars, 20 µm. Effectiveness of inhibition of the growth of the human cancer cell line MCF-7 (IC_{50} index); and lipid droplet formation (EC_{50} index) by Buclizine and its analogue **94**. HATU, 1-(*bis*(dimethylamino)methylene)-1*H*-1,2,3-triazolo(4,5-b)pyridinium 3-oxid hexafluorophosphate; DMSO, dimethyl sulfoxide.

followed by the resazurin reduction assay. Buclizine also induced cell differentiation, which was seen in an accumulation of intracellular lipid droplets. In this work, we tested analogue **94**, for its ability to arrest cell growth and induce lipid droplets and compared it to the parent Buclizine molecule (for details, see Supplementary Information, pages 886–889). By doing so, we expected to characterize indirectly the interaction of the compounds with the tumour protein depending on the presence of an isostere in the molecule.

In the resazurin reduction assay, the original drug, Buclizine, showed moderate effectiveness (half-maximum inhibitory concentration (IC_{50}) 31.3 ± 7.8 µM; Fig. 7). The BCP analogue **94** behaved similarly (IC_{50} = 24.5 ± 1.5 µM). In an experiment assisted by fluorescence imaging, Buclizine (half-maximum effective concentration (EC_{50}) 19 µM) and the BCP analogue **94** (EC_{50} = 16 µM) also showed a similar onset of lipid droplet formation.

This overall preservation of activity in both analogues **91** (Benzocaine) and **94** (Buclizine) demonstrates that the benzene-to-BCP replacement is bioisosteric, thus supporting the literature data[4–8].

Summary

In 2012, BCPs were demonstrated to mimic the benzene ring in bioactive compounds[4]. Here, we report a general scalable reaction between alkyl iodides and propellane that gives alkyl-substituted BCP iodides in milligram, gram and even kilogram quantities. The reaction proceeds in flow and requires only light. No catalysts, initiators or additives are needed. The reaction is so clean that in many cases, evaporation of the reaction mixture provides products in around 90% purity that can be directly used in the next step without any purification. With the subsequent modifications, we have prepared >300 of BCPs for use in medicinal chemistry. So far, this is the most general and scalable approach towards functionalized BCPs.

We hope that this work will help process chemists at pharmaceutical companies with the preparation of bioactive BCPs suggested by medicinal chemists for clinical trials.

Methods

Synthesis of 3-iodo-BCPs and 3-iodobicyclo[3.1.1]heptanes

General protocol A. To a solution of MeI (10.00 g, 0.0704 mol, 1.00 equiv.) in Et_2O (100 ml), was added propellane (120 ml, 0.0840 mol, 0.7 M solution in Et_2O–diethoxymethane; 1.20 equiv.) under an argon atmosphere. The resulting mixture was passed through a photoreactor. The flow rate was 10 ml min^{-1}; the irradiated coil was 160 ml, irradiation was 365 nm, LED, and the irradiated power was 420 W (50% of the maximal). Before entering the irradiated area, the solution was precooled to 0 °C with Huber Unistat 510 chiller. The irradiated coil was also cooled to 0 °C with Huber Unistat 510 chiller. The temperature of the reaction mixture after the coil was around 10 °C. After passing through the coil, after around 40 min (residence time in the irradiated coil, 160/10 approximately 16 min) the solution was evaporation under a reduced pressure (around 50 mmHg, 20 °C in an external water-cooling bath), and the residue was purified by distillation under a reduced pressure (boiling point 38–40 °C at 10 mmHg). After cooling down to room temperature, the product **1** (9.21 g, 0.0438 mol, yield 62%) slowly solidified. Alternatively, the crude residue (after evaporation of the reaction mixture after the irradiation) could be purified by adding pentane (around 50 ml) and cooling the formed suspension with an external dry ice bath to around −60 °C. The formed precipitate was quickly filtered off. The filtered solid was washed with the precooled pentane (−60 °C, 50 ml) on the filter, and was dried under vacuum (20 mmHg) during 30 min at room temperature. Yield was 9.77 g, 0.0465 mol, 66%, white crystals, melting point <30 °C.

NMR spectra were analysed with MestreNova (v.11.0.3-18688).

Reporting summary

Further information on research design is available in the Nature Portfolio Reporting Summary linked to this article.

Data availability

The data underlying this study are available in the published article and its Supplementary Information, including experimental procedures, calculations, characterization data, copies of ^{1}H, ^{19}F, ^{13}C NMR spectra. Crystallographic data for the structures reported in this Article have been deposited at the Cambridge Crystallographic Data Centre, under deposition numbers CCDC 2260408 (**14**), 2244857 (**19**), 2244859 (**55**), 2237112 (**2k**) and 2244856 (**21k**). Copies of the data can be obtained free of charge via https://www.ccdc.cam.ac.uk/structures/.

References

1. Taylor, R. D., MacCoss, M. & Lawson, A. D. G. Rings in drugs. *J. Med. Chem.* **57**, 5845–5859 (2014).
2. Shearer, J., Castro, J. L., Lawson, A. D. G., MacCoss, M. & Taylor, R. D. Rings in clinical trials and drugs: present and future. *J. Med. Chem.* **65**, 8699–8712 (2022).
3. Chen, Y., Rosenkranz, C., Hirte, S. & Kirchmair, J. Ring systems in natural products: structural diversity, physicochemical properties, and coverage by synthetic compounds. *Nat. Prod. Rep.* **39**, 1544–1556 (2022).
4. Stepan, A. F. et al. Application of the bicyclo[1.1.1]pentane motif as a nonclassical phenyl ring bioisostere in the design of a potent and orally active γ-secretase inhibitor. *J. Med. Chem.* **55**, 3414–3424 (2012).
5. Mykhailiuk, P. K. Saturated bioisosteres of benzene: where to go next? *Org. Biomol. Chem.* **17**, 2839–2849 (2019).
6. Locke, G. M., Bernhard, S. S. R. & Senge, M. O. Nonconjugated hydrocarbons as rigid-linear motifs: isosteres for material sciences and bioorganic and medicinal chemistry. *Chem. Eur. J.* **25**, 4590–4647 (2019).
7. Macreadie, L. K., Idrees, K. B., Smoljan, C. S. & Farha, O. K. Expanding linker dimensionality in metal-organic frameworks for sub-Ångstrom pore control for separation applications. *Angew. Chem. Int. Ed.* **62**, e202304094 (2023).
8. Subbaiah, M. A. M. & Meanwell, N. A. Bioisosteres of the phenyl ring: recent strategic applications in lead optimization and drug design. *J. Med. Chem.* **64**, 14046–14128 (2021).
9. Kanazawa, J. & Uchiyama, M. Recent advances in the synthetic chemistry of bicyclo[1.1.1]pentane. *Synlett* **30**, 1–11 (2019).
10. Ma, X. & Pham, L. N. Selected topics in the syntheses of bicyclo[1.1.1]pentane (BCP) analogues. *Asian J. Org. Chem.* **9**, 8–22 (2020).
11. He, F.-S., Xie, S., Yao, Y. & Wu, J. Recent advances in the applications of [1.1.1]propellane in organic synthesis. *Chin. Chem. Lett.* **31**, 3065–3072 (2020).
12. Anderson, J. M., Measom, N. D., Murphy, J. A. & Poole, D. L. Bridge functionalisation of bicyclo[1.1.1]pentane derivatives. *Angew. Chem. Int. Ed.* **60**, 24754–24769 (2021).
13. Shire, B. R. & Anderson, E. A. Conquering the synthesis and functionalization of bicyclo[1.1.1]pentanes. *JACS Au* **3**, 1539–1553 (2023).
14. Bellotti, P. & Glorius, F. Strain-release photocatalysis. *J. Am. Chem. Soc.* **145**, 20716–20732 (2023).
15. Nicolaou, K. C. et al. Synthesis and biopharmaceutical evaluation of imatinib analogues featuring unusual structural motifs. *Chem. Med. Chem.* **11**, 31–37 (2016).
16. Measom, N. D. et al. Investigation of a bicyclo[1.1.1]pentane as a phenyl replacement within an $LpPLA_2$ inhibitor. *ACS Med. Chem. Lett.* **8**, 43–48 (2017).
17. Goh, Y. L., Cui, Y. T., Pendharkar, V. & Adsool, V. A. Toward resolving the resveratrol conundrum: synthesis and in vivo pharmacokinetic evaluation of BCP–resveratrol. *ACS Med. Chem. Lett.* **8**, 516–520 (2017).
18. Pu, Q. et al. Discovery of potent and orally available bicyclo[1.1.1] pentane-derived indoleamine-2,3-dioxygenase 1 (IDO1) inhibitors. *ACS Med. Chem. Lett.* **11**, 1548–1554 (2020).
19. Mikhailiuk, P. K. et al. Conformationally rigid trifluoromethyl-substituted α-amino acid designed for peptide structure analysis by solid-state ^{19}F NMR spectroscopy. *Angew. Chem. Int. Ed.* **45**, 5659–5661 (2006).
20. Kokhan, S. O. et al. Design, synthesis, and application of an optimized monofluorinated aliphatic label for peptide studies by solid-state ^{19}F NMR spectroscopy. *Angew. Chem. Int. Ed.* **55**, 14788–14792 (2016).
21. Mykhailiuk, P. K., Voievoda, N. M., Afonin, S., Ulrich, A. S. & Komarov, I. V. An optimized protocol for the multigram synthesis of 3-(trifluoromethyl)bicyclo[1.1.1]pent-1-ylglycine (CF_3-Bpg). *J. Fluorine Chem.* **131**, 217–220 (2010).
22. Yang, B. et al. On-surface synthesis of polyphenylene wires comprising rigid aliphatic bicyclo[1.1.1]pentane isolator units. *Angew. Chem. Int. Ed.* **62**, e202218211 (2023).
23. Grover, N. et al. Bicyclo[1.1.1]pentane embedded in porphyrinoids. *Angew. Chem. Int. Ed.* **62**, e202302771 (2023).
24. Ma, X., Han, Y. & Bennett, D. J. Selective synthesis of 1-dialkylamino-2-alkylbicyclo-[1.1.1]pentanes. *Org. Lett.* **22**, 9133–9138 (2020).
25. Zhao, J.-X. et al. 1,2-Difunctionalized bicyclo[1.1.1]pentanes: long–sought-after mimetics for ortho/meta-substituted arenes. *Proc. Natl Acad. Sci. USA* **118**, e2108881118 (2020).
26. Yang, Y. et al. An intramolecular coupling approach to alkyl bioisosteres for the synthesis of multisubstituted bicycloalkyl boronates. *Nat. Chem.* **13**, 950–955 (2021).
27. Ma, X., Sloman, D. L., Han, Y. & Bennett, D. J. A selective synthesis of 2,2-difluorobicyclo[1.1.1]pentane analogues: 'BCP-F_2'. *Org. Lett.* **21**, 7199–7203 (2019).
28. Bychek, R. M. et al. Difluoro-substituted bicyclo[1.1.1]pentanes for medicinal chemistry: design, synthesis, and characterization. *J. Org. Chem.* **84**, 15106–15117 (2019).
29. Anderson, J. M., Measom, N. D., Murphy, J. A. & Poole, D. L. Bridge heteroarylation of bicyclo[1.1.1]pentane derivatives. *Org. Lett.* **25**, 2053–2057 (2023).
30. Bychek, R. & Mykhailiuk, P. K. A practical and scalable approach to fluoro-substituted bicyclo[1.1.1]pentanes. *Angew. Chem. Int. Ed.* **61**, e202205103 (2022).
31. Garry, O. L. et al. Rapid access to 2-substituted bicyclo[1.1.1] pentanes. *J. Am. Chem. Soc.* **145**, 3092–3100 (2023).
32. Wright, B. A. et al. Skeletal editing approach to bridge-functionalized bicyclo[1.1.1]pentanes from azabicyclo[2.1.1]hexanes. *J. Am. Chem. Soc.* **145**, 10960–10966 (2023).
33. Gianatassio, R. et al. Strain-release amination. *Science* **351**, 241–246 (2016).
34. Lopchuk, J. M. et al. Strain-release heteroatom functionalization: development, scope, and stereospecificity. *J. Am. Chem. Soc.* **139**, 3209–3226 (2017).
35. Lovering, F., Bikker, J. & Humblet, C. Escape from Flatland: increasing saturation as an approach to improving clinical success. *J. Med. Chem.* **52**, 6752–6756 (2009).
36. Lovering, F. Escape from Flatland 2: complexity and promiscuity. *Med. Chem. Commun.* **4**, 515–519 (2013).
37. Kaszynski, P., McMurdie, N. D. & Michl, J. Synthesis of doubly bridgehead substituted bicyclo[1.1.1]pentanes. Radical transformations of bridgehead halides and carboxylic acids. *J. Org. Chem.* **56**, 307–316 (1991).

38. Messner, M., Kozhushkov, S. I. & de Meijere, A. Nickel- and palladium-catalyzed cross-coupling reactions at the bridgehead of bicyclo[1.1.1]pentane derivatives—a convenient access to liquid crystalline compounds containing bicyclo[1.1.1]pentane moieties. *Eur. J. Org. Chem*. **2000**, 1137–1155 (2000).
39. Kaszynski, P., Friedli, A. C. & Michl, J. Toward a molecular-size tinkertoy construction set. Preparation of terminally functionalized [n]staffanes from [1.1.1]propellane. *J. Am. Chem. Soc*. **114**, 601–620 (1992).
40. Wiberg, K. B. & McMurdie, N. Formation and reactions of bicyclo[1.1.1]pentyl-1 cations. *J. Am. Chem. Soc*. **116**, 11990–11998 (1994).
41. Vyas, V. K., Clarkson, G. J. & Wills, M. Enantioselective synthesis of bicyclopentane-containing alcohols via asymmetric transfer hydrogenation. *Org. Lett*. **23**, 3179–3183 (2021).
42. Dron, P. I. et al. Bulk inclusions of pyridazine-based molecular rotors in tris(o-phenylenedioxy)cyclotriphosphazene (TPP). *Adv. Funct. Mater*. **26**, 5718–5732 (2016).
43. Kaleta, J., Nečas, M. & Mazal, C. 1,3-Diethynylbicyclo[1.1.1]pentane, a useful molecular building block. *Eur. J. Org. Chem*. **25**, 4783–4796 (2012).
44. Caputo, D. F. J. et al. Synthesis and applications of highly functionalized 1-halo-3-substituted bicyclo[1.1.1]pentanes. *Chem. Sci*. **9**, 5295–5390 (2018).
45. Wong, M. L. J., Mousseau, J. J., Mansfield, S. J. & Anderson, E. A. Synthesis of enantioenriched α-chiral bicyclo[1.1.1]pentanes. *Org. Lett*. **21**, 2408–2411 (2019).
46. Pickford, H. D. et al. Twofold radical-based synthesis of N,C-difunctionalized bicyclo[1.1.1]pentanes. *J. Am. Chem. Soc*. **143**, 9729–9736 (2021).
47. Nugent, J. et al. A general route to bicyclo[1.1.1]pentanes through photoredox catalysis. *ACS Catal*. **9**, 9568–9574 (2019).
48. Yen-Pon, E. et al. On-DNA hydroalkylation to introduce diverse bicyclo[1.1.1]pentanes and abundant alkyls via halogen atom transfer. *J. Am. Chem. Soc*. **144**, 12184–12191 (2022).
49. Adcock, J. L. & Gakh, A. A. Nucleophilic substitution in 1-substituted 3-iodobicyclo[1.1.1]pentanes. A new synthetic route to functionalized bicyclo[1.1.1]pentane derivatives. *J. Org. Chem*. **57**, 6206–6210 (1992).
50. Krishnan, A., Robert, J., Qinhua, P. & Duane, K. Difluoromethyl iodo compounds and methods. WO2021167987A1 (2021).
51. Deng, G., Yao, Y., Liu, X., Li, Z., Dai, M., Huan, R., Tang, R., Huang, D., Zhang, Q., Wang, Y., Ye, Y. & Peng, J. Preparation method for bicyclic compound and application as antifungal agent. WO2022206862A1 (2022).
52. Pirali, T., Serafini, M., Cargnin, S. & Genazzani, A. A. Applications of deuterium in medicinal chemistry. *J. Med. Chem*. **62**, 5276–5297 (2019).
53. Di Martino, R. M. C., Maxwell, B. D. & Pirali, T. Deuterium in drug discovery: progress, opportunities and challenges. *Nat. Rev. Drug. Discov*. **22**, 562–584 (2023).
54. Gillis, E. P., Eastman, K. J., Hill, M. D., Donnelly, D. J. & Meanwell, N. A. Applications of fluorine in medicinal chemistry. *J. Med. Chem*. **58**, 8315–8359 (2015).
55. Meanwell, N. A. Fluorine and fluorinated motifs in the design and application of bioisosteres for drug design. *J. Med. Chem*. **61**, 5822–5880 (2018).
56. Inoue, M., Sumii, Y. & Shibata, N. Contribution of organofluorine compounds to pharmaceuticals. *ACS Omega* **5**, 10633–10640 (2020).
57. Levterov, V. V., Panasyuk, Y., Pivnytska, V. O. & Mykhailiuk, P. K. Water-soluble non-classical benzene mimetics. *Angew. Chem. Int. Ed*. **59**, 7161–7167 (2020).
58. Levterov, V. V. et al. 2-Oxabicyclo[2.1.1]hexanes: synthesis, properties and validation as bioisosteres of ortho- and meta-Benzenes. *Angew. Chem. Int. Ed*. **63**, e202319831 (2024).
59. Denisenko, A., Garbuz, P., Voloshchuk, N. M., Holota, Y. & Mykhailiuk, P. K. 2-Oxabicyclo[2.1.1]hexanes as saturated bioisosteres of the ortho-substituted phenyl ring. *Nat. Chem*. **15**, 1155–1163 (2023).
60. Fominova, K. et al. Oxa-spirocycles: synthesis, properties and applications. *Chem. Sci*. **12**, 11294–11305 (2021).
61. Rentería-Gómez, A. et al. General and practical route to diverse 1-(difluoro)alkyl-3-aryl bicyclo[1.1.1]pentanes enabled by an Fe-catalyzed multicomponent radical cross-coupling reaction. *ACS Catal*. **12**, 11547–11556 (2022).
62. Cuadros, S. et al. A general organophotoredox strategy to difluoroalkyl bicycloalkane (CF_2-BCA) hybrid bioisosteres. *Angew. Chem. Int. Ed*. **62**, e202303585 (2023).
63. Frank, N. et al. Synthesis of meta-substituted arene bioisosteres from [3.1.1]propellane. *Nature* **611**, 721–726 (2022).
64. Griller, D. & Ingold, K. U. Free-radical clocks. *Acc. Chem. Res*. **13**, 317–323 (1980).
65. Fawcett, A. et al. Photoinduced decarboxylative borylation of carboxylic acids. *Science* **357**, 283–286 (2017).
66. Wang, J. et al. Cu-catalyzed decarboxylative borylation. *ACS Catal*. **8**, 9537–9542 (2018).
67. Kondo, M. et al. Silaboration of [1.1.1]propellane: storable feedstock for bicyclo[1.1.1]pentane derivatives. *Angew. Chem. Int. Ed*. **59**, 1970–1974 (2020).
68. Zhang, Q. et al. Decarboxylative borylation of stabilized and activated carbon radicals. *Angew. Chem. Int. Ed*. **59**, 21875–21879 (2020).
69. VanHeyst, M. D. et al. Continuous flow-enabled synthesis of bench-stable bicyclo[1.1.1]pentane trifluoroborate salts and their utilization in metallaphotoredox cross-couplings. *Org. Lett*. **22**, 1648–1654 (2020).
70. Shelp, R. A. et al. Strain-release 2-azaallyl anion addition/borylation of [1.1.1]propellane: synthesis and functionalization of benzylamine bicyclo[1.1.1]pentyl boronates. *Chem. Sci*. **12**, 7066–7072 (2021).
71. Zarate, C. et al. Development of scalable routes to 1-bicyclo[1.1.1]pentylpyrazoles. *Org. Process Res. Dev*. **25**, 642–647 (2021).
72. Barton, L. M., Chen, L., Blackmond, D. G. & Baran, P. S. Electrochemical borylation of carboxylic acids. *Proc. Natl Acad. Sci. USA* **118**, e2109408118 (2021).
73. Dong, W. et al. Exploiting the sp^2 character of bicyclo[1.1.1]pentyl radicals in the transition-metal-free multi-component difunctionalization of [1.1.1]propellane. *Nat. Chem*. **14**, 1068–1077 (2022).
74. Alvarez, E. M. et al. O-, N- and C-bicyclopentylation using thianthrenium reagents. *Nat. Synth*. **2**, 548–556 (2023).
75. Bunker, K. D., Sach, N. W., Huang, Q. & Richardson, P. F. Scalable synthesis of 1-bicyclo[1.1.1]pentylamine via a hydrohydrazination reaction. *Org. Lett*. **13**, 4746–4748 (2011).
76. Kanazawa, J., Maeda, K. & Uchiyama, M. Radical multicomponent carboamination of [1.1.1]propellane. *J. Am. Chem. Soc*. **139**, 17791–17794 (2017).
77. Bär, R. M., Kirschner, S., Nieger, M. & Bräse, S. Alkyl and aryl thiol addition to [1.1.1]propellane: scope and limitations of a fast conjugation reaction. *Chem. Eur. J*. **24**, 1373–1382 (2018).
78. Kraemer, Y. et al. Strain-release pentafluorosulfanylation and tetrafluoro(aryl)sulfanylation of [1.1.1]propellane: reactivity and structural insight. *Angew. Chem. Int. Ed*. **61**, e202211892 (2022).
79. Livesley, S. et al. Synthesis of sulfur-substituted bicyclo[1.1.1]pentanes by iodo-sulfenylation of [1.1.1]propellane. *Org. Lett*. **24**, 7015–7020 (2022).

80. Pickford, H. D. et al. Rapid and scalable halosulfonylation of strain-release reagents. *Angew. Chem. Int. Ed.* **62**, e202213508 (2023).
81. Dong, W., Keess, S. & Molander, G. A. Nickel-mediated alkyl-, acyl-, and sulfonylcyanation of [1.1.1]propellane. *Chem. Catalysis* **3**, 100608 (2023).
82. Makarov, I. S., Brocklehurst, C. E., Karaghiosoff, K., Koch, G. & Knochel, P. Synthesis of bicyclo[1.1.1]pentane bioisosteres of internal alkynes and *para*-disubstituted benzenes from [1.1.1] propellane. *Angew. Chem. Int. Ed.* **56**, 12774–12777 (2017).
83. Shelp, R. A. & Walsh, P. J. Synthesis of BCP benzylamines from 2-azaallyl anions and [1.1.1]propellane. *Angew. Chem. Int. Ed.* **57**, 15857–15861 (2018).
84. Trongsiriwat, N. et al. Reactions of 2-aryl-1,3-dithianes and [1.1.1]propellane. *Angew. Chem. Int. Ed.* **58**, 13416–13420 (2019).
85. Yu, S., Jing, C., Noble, A. & Aggarwal, V. K. 1,3-Difunctionalizations of [1.1.1]propellane via 1,2-metallate rearrangements of boronate complexes. *Angew. Chem. Int. Ed.* **59**, 3917–3921 (2020).
86. Schwärzer, K., Zipse, H., Karaghiosoff, K. & Knochel, P. Highly regioselective addition of allylic zinc halides and various zinc enolates to [1.1.1]propellane. *Angew. Chem. Int. Ed.* **59**, 20235–20241 (2020).
87. Garlets, Z. J. et al. Functionalization of bicyclo[1.1.1]pentanes. *Nat. Catal.* **3**, 351–357 (2020).
88. Yu, S., Jing, C., Noble, A. & Aggarwal, V. K. Iridium-catalyzed enantioselective synthesis of α-chiral bicyclo[1.1.1]pentanes by 1,3-difunctionalization of [1.1.1]propellane. *Org. Lett.* **22**, 5650–5655 (2020).
89. Andersen, C. et al. Copper-catalyzed cross-coupling between alkyl (pseudo)halides and bicyclopentyl Grignard reagents. *Org. Lett.* **22**, 6021–6025 (2020).
90. Wong, M. L. J., Sterling, A. J., Mousseau, J. J., Duarte, F. & Anderson, E. A. Direct catalytic asymmetric synthesis of α-chiral bicyclo[1.1.1]pentanes. *Nat. Commun.* **12**, 1644 (2021).
91. Polites, V. C., Badir, S. O., Keess, S., Jolit, A. & Molander, G. A. Nickel-catalyzed decarboxylative cross-coupling of bicyclo[1.1.1] pentyl radicals enabled by electron donor-acceptor complex photoactivation. *Org. Lett.* **23**, 4828–4833 (2021).
92. Nugent, J., Sterling, A. J., Frank, N., Mousseau, J. J. & Anderson, E. A. Synthesis of *α*-quaternary bicyclo[1.1.1]pentanes through synergistic organophotoredox and hydrogen atom transfer catalysis. *Org. Lett.* **23**, 8628–8633 (2021).
93. Mousseau, J. J. et al. Automated nanomole-scale reaction screening toward benzoate bioisosteres: a photocatalyzed approach to highly elaborated bicyclo[1.1.1]pentanes. *ACS Catal.* **12**, 600–606 (2022).
94. Huang, W., Keess, S. & Molander, G. A. One step synthesis of unsymmetrical 1,3-disubstituted BCP ketones via nickel/photoredoxcatalyzed [1.1.1]propellane multicomponent dicarbofunctionalization. *Chem. Sci.* **13**, 11936–11942 (2022).
95. Huang, W., Keess, S. & Molander, G. A. Dicarbofunctionalization of [1.1.1]propellane enabled by nickel/photoredox dual catalysis: one-step multicomponent strategy for the synthesis of BCP-aryl derivatives. *J. Am. Chem. Soc.* **144**, 12961–12969 (2022).
96. Shelp, R., Merchant, R. R., Hughes, J. M. E. & Walsh, P. J. Enantioenriched BCP benzylamine synthesis via metal hydride hydrogen atom transfer/sulfinimine addition to [1.1.1]propellane. *Org. Lett.* **24**, 110–114 (2022).
97. Li, Q., Li, L., Xu, Q.-L. & Pan, F. Radical acylation of [1.1.1]propellane with aldehydes: synthesis of bicyclo[1.1.1]pentane ketones. *Org. Lett.* **24**, 4292–4297 (2022).
98. Huang, W., Keess, S. & Molander, G. A. A general and practical route to functionalized BCP-heteroaryls enabled by photocatalytic multicomponent heteroarylation of [1.1.1] propellane. *Angew. Chem. Int. Ed.* **62**, e202302223 (2023).
99. Gao, Y. et al. Visible light-induced synthesis of 1,3-disubstituted bicyclo[1.1.1]pentane ketones via cooperative photoredox and N-heterocyclic carbene catalysis. *Green Chem.* **25**, 3909–3915 (2023).
100. Ripenko, V., Vysochyn, D., Klymov, I., Zhersh, S. & Mykhailiuk, P. K. Large-scale synthesis and modifications of bicyclo[1.1.1]pentane-1,3-dicarboxylic acid (BCP). *J. Org. Chem.* **86**, 14061–14068 (2021).
101. Huang, W., Zheng, Y., Keess, S. & Molander, G. A. A general and modular approach to BCP alkylamines via multicomponent difunctionalization of [1.1.1]propellane. *J. Am. Chem. Soc.* **145**, 5363–5369 (2023).
102. Hughes, J. M. E., Scarlata, D. A., Chen, A. C.-Y., Burch, J. D. & Gleason, J. L. Aminoalkylation of [1.1.1]propellane enables direct access to high-value 3-alkylbicyclo[1.1.1]pentan-1-amines. *Org. Lett.* **21**, 6800–6804 (2019).
103. Kim, J. H., Ruffoni, A., Al-Faiyz, Y. S. S., Sheikh, N. S. & Leonori, D. Divergent strain-release amino-functionalization of [1.1.1] propellane with electrophilic nitrogen-radicals. *Angew. Chem. Int. Ed.* **59**, 8225–8231 (2020).
104. Zhang, X. et al. Copper-mediated synthesis of drug-like bicyclopentanes. *Nature* **580**, 220–226 (2020).
105. Shin, S., Lee, S., Choi, W., Kim, N. & Hong, S. Visible-light-induced 1,3-aminopyridylation of [1.1.1]propellane with *n*-aminopyridinium salts. *Angew. Chem. Int. Ed.* **60**, 7873–7879 (2021).
106. Livesley, S. et al. Electrophilic activation of [1.1.1]propellane for the synthesis of nitrogen-substituted bicyclo[1.1.1]pentanes. *Angew. Chem. Int. Ed.* **61**, e202111291 (2022).
107. Nugent, J. et al. Synthesis of all-carbon disubstituted bicyclo[1.1.1] pentanes by iron-catalyzed Kumada cross-coupling. *Angew. Chem. Int. Ed.* **59**, 11866–11870 (2020).
108. Alonso, M. et al. Accelerated synthesis of bicyclo[1.1.1]pentylamines: a high-throughput approach. *Org. Lett.* **25**, 771–776 (2023).
109. Davies, O. L., Raventós, J. A. & Walpole, L. A method for the evaluation of analgesic activity using rats. *Br. J. Pharmacol Chemother*. **1**, 255–264 (1946).
110. Seo, E.-J. & Efferth, T. Interaction of antihistaminic drugs with human translationally controlled tumor protein (TCTP) as novel approach for differentiation therapy. *Oncotarget*. **7**, 16818–16839 (2016).

Acknowledgements

This project has received funding from the European Research Council under the European Union's Horizon 2020 research and innovation programme (grant agreement no. 101000893 - BENOVELTY). P.M. is also grateful to S. Shishkina (Institute of Organic Chemistry, Kyiv) for X-ray studies, D. Bylina (Enamine) for high resolution mass spectrometry (HRMS) measurements, Y. Holota (Bienta) for the help with measurements of physico-chemical properties, P. Borysko (Bienta) with the managing help with biological experiments, V. Kubyshkin (Enamine) for the help in the preparation of the manuscript and to I. Stadnyi (Enamine) and M. Kucherbaev (Enamine) for the assistance with the photoreactors.

Author contributions

V.R., V.S., S.Z. and P.K.M. designed the experiments. V.R., V.S., V.L., S.H., D.V., I.K., D.K., S.V., Y.D., A.T., I.S., I.P., K.H., V.K. and Y.N. conducted and analysed the experiments described in this report. P.K.M. and I.S. prepared this manuscript for publication.

Competing interests

The authors declare the following competing interests: V.R., V.S., V.L., S.H., D.V., I.K., D.K., S.V., S.Z., Y.D., A.T., I.S. and P.K.M. are employees of a chemical supplier, Enamine. The remaining authors declare no competing interests.

Additional information

Supplementary information The online version contains supplementary material available at https://doi.org/10.1038/s44160-024-00637-y.

Correspondence and requests for materials should be addressed to Pavel K. Mykhailiuk.

Peer review information *Nature Synthesis* thanks Murugaiah Subbaia and the other, anonymous, reviewer(s) for their contribution to the peer review of this work. Primary Handling Editor: Peter Seavill, in collaboration with the *Nature Synthesis* team.

nature research

Corresponding author(s): Pavel K. Mykhailiuk

Last updated by author(s): Jul 24, 2024

Reporting Summary

Nature Research wishes to improve the reproducibility of the work that we publish. This form provides structure for consistency and transparency in reporting. For further information on Nature Research policies, see our Editorial Policies and the Editorial Policy Checklist.

Statistics

For all statistical analyses, confirm that the following items are present in the figure legend, table legend, main text, or Methods section.

n/a	Confirmed	
☐	☒	The exact sample size (*n*) for each experimental group/condition, given as a discrete number and unit of measurement
☐	☒	A statement on whether measurements were taken from distinct samples or whether the same sample was measured repeatedly
☐	☒	The statistical test(s) used AND whether they are one- or two-sided *Only common tests should be described solely by name; describe more complex techniques in the Methods section.*
☒	☐	A description of all covariates tested
☒	☐	A description of any assumptions or corrections, such as tests of normality and adjustment for multiple comparisons
☐	☒	A full description of the statistical parameters including central tendency (e.g. means) or other basic estimates (e.g. regression coefficient) AND variation (e.g. standard deviation) or associated estimates of uncertainty (e.g. confidence intervals)
☐	☒	For null hypothesis testing, the test statistic (e.g. *F*, *t*, *r*) with confidence intervals, effect sizes, degrees of freedom and *P* value noted *Give P values as exact values whenever suitable.*
☒	☐	For Bayesian analysis, information on the choice of priors and Markov chain Monte Carlo settings
☒	☐	For hierarchical and complex designs, identification of the appropriate level for tests and full reporting of outcomes
☒	☐	Estimates of effect sizes (e.g. Cohen's *d*, Pearson's *r*), indicating how they were calculated

Our web collection on statistics for biologists contains articles on many of the points above.

Software and code

Policy information about availability of computer code

Data collection	Product purification was performed using HPLC AGILENT 1260 INFINITY (a column Chromatorex C18 SMB 100-5T, 100*19 mm, 5 microm) or PuriFlash XS420 Plus. The NMR data acquisition was performed using Varian UNITY III 400; Varian VNMRS 500; Bruker AVANCE DRX 500 and Bruker AVANCE III 400 spectrometers. HRMS data acquisition was performed using Agilent 6224 TOF LC/MS. Lipophilicity (clogP) was calculated with "Cxcalc" ChemAxon, version 22.5.0. Microscopy data were acquired using InCell Analyzer 6500HS (Cytiva)
Data analysis	The NMR data analysis was performed using Mestrenova software (11.0.3-18688). The data acquisition and system control was performed using Analyst 1.6.3 software from AB Sciex. Microscopy images analysis was performed with InCarta 1.13 (Cytiva). Data analysis of biochemical and cell based experiments was performed using GraphPad Prism 9.

For manuscripts utilizing custom algorithms or software that are central to the research but not yet described in published literature, software must be made available to editors and reviewers. We strongly encourage code deposition in a community repository (e.g. GitHub). See the Nature Research guidelines for submitting code & software for further information.

Data

Policy information about availability of data

All manuscripts must include a data availability statement. This statement should provide the following information, where applicable:

- Accession codes, unique identifiers, or web links for publicly available datasets
- A list of figures that have associated raw data
- A description of any restrictions on data availability

Experimental data as well as characterization data for all new compounds prepared during these studies are provided in the Supplementary Information of this

manuscript. Crystallographic data for the structures reported in this Article have been deposited at the Cambridge Crystallographic Data Centre, under deposition numbers CCDC 2260408 (14), 2244857 (19), 2244859 (55), 2237112 (2k) and 2244856 (21k). Copies of the data can be obtained free of charge via https://www.ccdc.cam.ac.uk/structures/.

Field-specific reporting

Please select the one below that is the best fit for your research. If you are not sure, read the appropriate sections before making your selection.

☒ Life sciences ☐ Behavioural & social sciences ☐ Ecological, evolutionary & environmental sciences

For a reference copy of the document with all sections, see nature.com/documents/nr-reporting-summary-flat.pdf

Life sciences study design

All studies must disclose on these points even when the disclosure is negative.

Sample size	Cell-based assays: n = 3, independent wells, for every of which approx. 2000 visualised cells were analyzed.
Data exclusions	No data were excluded from the analysis.
Replication	3 replicates across independent wells.
Randomization	The completely randomized design (CRD) was used for all in vitro experiments. It is appropriate in situations in which the material is genetically and physiologically homogeneous (stable cell culture and recombinant protein), and all assays had been performed within a corresponding single assay plate for each type of experiment.
Blinding	Compared items and reference compund(s) are provided to the researcher in 96- or 384- well plates by separate department. Plate maps are not available for the researcher.

Reporting for specific materials, systems and methods

We require information from authors about some types of materials, experimental systems and methods used in many studies. Here, indicate whether each material, system or method listed is relevant to your study. If you are not sure if a list item applies to your research, read the appropriate section before selecting a response.

Materials & experimental systems

n/a	Involved in the study
☒	☐ Antibodies
☐	☒ Eukaryotic cell lines
☒	☐ Palaeontology and archaeology
☒	☐ Animals and other organisms
☒	☐ Human research participants
☒	☐ Clinical data
☒	☐ Dual use research of concern

Methods

n/a	Involved in the study
☒	☐ ChIP-seq
☒	☐ Flow cytometry
☒	☐ MRI-based neuroimaging

Eukaryotic cell lines

Policy information about cell lines

Cell line source(s)	DSMZ: ACC-180 https://celldive.dsmz.de/cellline/ACC-180
Authentication	The cell line was not authenticated, as obtained from the commercial source.
Mycoplasma contamination	All cells tested negative for mycoplasma contamination by MycoSEQ™ Mycoplasma Detection Kits Applied Biosystems™ Catalog number: 4460626
Commonly misidentified lines (See ICLAC register)	n/a